Two-component Fermi gas in a one-dimensional harmonic trap

Gao Xianlong and W. Wonneberger
Abteilung für Mathematische Physik, Universität Ulm, D89069 Ulm, Germany
(Received 28 August 2001; published 8 February 2002)

A many-body theory for a two-component system of spin-polarized interacting fermions in a one-dimensional harmonic trap is developed. The model considers two different states of the same fermionic species and treats the dominant interactions between the two using the bosonization method for forward scattering. Asymptotically exact results for the one-particle matrix elements at zero temperature are given. Using them, occupation probabilities of oscillator states are discussed. Particle and momentum densities are calculated and displayed. It is demonstrated how interactions modify all these quantities. An asymptotic connection with Luttinger liquids is suggested. The relation of the coupling constant of the theory to the dipole-dipole interaction is also discussed.

DOI: 10.1103/PhysRevA.65.033610 PACS number(s): 03.75.Fi, 05.30.Fk, 71.10.Pm

I. INTRODUCTION

The achievement of Bose-Einstein condensation in dilute ultracold gases [1] renewed the interest in fermionic many-body systems [2–4] and their superfluid properties [5–8]. Recent experimental successes in obtaining degeneracy in three-dimensional Fermi vapors [9,10] intensified the interest in confined Fermi gases. Using microtrap technology [11–14], it will become possible in the near future to produce a neutral ultracold quantum gas of quasi-one-dimensional degenerate fermions.

In many cases, identical spin-polarized fermions experience only a weak residual interaction because *s*-wave scattering is forbidden. This restriction does not hold for a two-component system of spin-polarized fermions and significant interactions between the components are possible. For instance, the dipole-dipole interaction [15] can become relevant, especially in the case of polar molecules [16].

The confinement of a trapped ultracold gas can be realized by a harmonic potential, which is more realistic than trapping between hard walls (‘‘open boundary conditions’’). The latter system of interacting one-dimensional fermions constitutes a bounded Luttinger liquid, which allows an exact treatment for certain types of interactions [17–23].

In this paper, we consider a quasi-one-dimensional spin-polarized Fermi gas composed of an equal number of atoms in two different internal states and confined by a harmonic potential. One possible realization consists of trapped (electron) spin-polarized fermions in two different hyperfine states, as discussed in [5] for the case of ^{6}Li.

We consider the intercomponent interaction between the two components. As in [24], we apply the bosonization method known from the Luttinger model (for reviews we refer to [25–27]) to treat the interactions. The generalization to two components is analogous to the inclusion of spin $\hbar/2$ into the Luttinger model [28]. The bosonization method relies on fermion-boson transmutation in one spatial dimension: Physical quantities can be calculated in a bosonic formulation instead of the fermionic theory, and the two calculations give the same answer [29–32].

We show how interactions modify the one-particle properties of the two-component Fermi gas. Results for the non-interacting Fermi gas in a one-dimensional harmonic trap were given in [33,34].

The paper is organized as follows. Section II develops the theory for the two-component case. Section III applies the theory to the calculation of the one-particle matrix elements. In Sec. IV, occupation probabilities, off-diagonal matrix elements, and densities of particles and momenta are evaluated numerically for two different interaction models. Section V discusses the problem of the Fermi edge in the present case, and a possible relation to the standard Luttinger model result is pointed out. In Sec. VI, the relation of the coupling constant of the theory to the dipole-dipole interaction is discussed. The Appendix is concerned with the bosonization procedure for bilinear forms of auxiliary fields in the case of two components.

II. TWO-COMPONENT THEORY

The two-component Fermi gas of uniform mass m_A is confined by the one-dimensional harmonic potential

$$V(z)=\frac{1}{2}m_A\omega_\ell^2 z^2, \tag{1}$$

with longitudinal trap frequency ω_ℓ. The unperturbed Hamiltonian in second quantization is

$$\hat{H}_0=\sum_{n=0,\sigma=\pm 1}^{\infty}\hbar\omega_n\hat{c}_{n\sigma}^{\dagger}\hat{c}_{n\sigma}. \tag{2}$$

The index $\sigma=\pm1$ refers to the two components and $\hat{c}_{n\sigma}^{\dagger}$ creates a fermion of species σ in the oscillator state $|n\rangle$.

The one-particle energies

$$\hbar\omega_n=\hbar\omega_\ell(n+1/2), \quad n=0,1,\ldots, \tag{3}$$

are seen to depend linearly on the quantum number n of oscillator states. This is one of the requirements for bosonization. In addition, exact solvability rests on the presence of an anomalous vacuum (cf. [25–27]), which is constructed by extending the linear dispersion of oscillator states to arbitrarily negative energies and then filling all states of negative energy. However, the anomalous vacuum has little effect for processes near the Fermi energy $\epsilon_F = \hbar\omega_\ell (N - 1/2)$ provided N is sufficiently large [32], making the treatment asymptotically exact.

The success of the Luttinger model is based on the possibility to express forward scattering processes entirely in terms of the density fluctuation operators. For the two-component system, these operators are

$$\hat{\rho}_\sigma(p) \equiv \sum_q \hat{c}^\dagger_{q+p\ \sigma} \hat{c}_{q\sigma}. \tag{4}$$

Due to the presence of the anomalous vacuum, they obey bosonic commutation relations

$$[\hat{\rho}_\sigma(-p), \hat{\rho}_{\sigma'}(q)] = p\ \delta_{\sigma,\sigma'} \delta_{p,q}. \tag{5}$$

In our case, the interaction Hamiltonian is given by a two-particle interaction

$$\hat{V} = \frac{1}{2} \sum_{mnpq,\sigma,\sigma'} V(m\sigma', p\sigma; q\sigma', n\sigma)\,(\hat{c}^\dagger_{m\sigma'} \hat{c}_{q\sigma'})(\hat{c}^\dagger_{p\sigma} \hat{c}_{n\sigma}) \tag{6}$$

without "component flip," i.e., the possibility for a fermion to change its state σ in the collision process is excluded.

The case $\sigma = \sigma'$ corresponds to a weak intracomponent interaction $V_\parallel$, while $\sigma = -\sigma'$ is a relevant intercomponent interaction $V_\perp$.

Similar to [24], two cases of solvable forward-scattering processes can be identified:

$$\hat{V} = \hat{V}_a + \hat{V}_b \tag{7}$$

with

$$\begin{aligned} \hat{V}_a &= \frac{1}{2} \sum_{p,\sigma} V_{a\parallel}(|p|) \hat{\rho}_\sigma(-p) \hat{\rho}_\sigma(p) + \frac{1}{2} \sum_{p,\sigma} V_{a\perp}(|p|) \\ &\quad \times \hat{\rho}_{-\sigma}(-p) \hat{\rho}_\sigma(p), \\ \hat{V}_b &= \frac{1}{2} \sum_{p,\sigma} V_{b\parallel}(|p|) \hat{\rho}_\sigma(p) \hat{\rho}_\sigma(p) \\ &\quad + \frac{1}{2} \sum_{p,\sigma} V_{b\perp}(|p|) \hat{\rho}_\sigma(p) \hat{\rho}_{-\sigma}(p). \end{aligned} \tag{8}$$

The coupling functions $V_{a\perp}$ and $V_{b\perp}$ are the analogs of $g_{4\perp}$ and $g_{2\perp}$ of the Luttinger model.

Forward scattering dominates when the pair interaction is sufficiently long-ranged, e.g., in the case of dipole-dipole interactions. In [35], a detailed discussion is given on how the assumed forms (8) can be related to real scattering potentials.

The case of two components requires canonical transformations to mass fluctuation operators

$$\hat{\rho}(p) \equiv \frac{1}{\sqrt{2}} [\hat{\rho}_+(p) + \hat{\rho}_-(p)] \tag{9}$$

and component fluctuation operators

$$\hat{\sigma}(p) \equiv \frac{1}{\sqrt{2}} [\hat{\rho}_+(p) - \hat{\rho}_-(p)], \tag{10}$$

such that the Hamiltonian for low-lying excitations separates into $\tilde{H} = \tilde{H}_\rho + \hat{H}_\sigma$ in analogy to the spin-$\frac{1}{2}$ case [28] of the Luttinger model.

The transformation to new bosonic operators

$$\hat{\rho}(p) = \begin{cases} \sqrt{|p|} & \hat{d}_{|p|+}, \quad p < 0, \\ \sqrt{p} & \hat{d}^\dagger_{p+}, \quad p > 0, \end{cases}$$

$$\hat{\sigma}(p) = \begin{cases} \sqrt{|p|} & \hat{d}_{|p|-}, \quad p < 0, \\ \sqrt{p} & \hat{d}^\dagger_{p-}, \quad p > 0, \end{cases} \tag{11}$$

leads to canonical commutation relations

$$[\hat{d}_{m\mu}, \hat{d}^\dagger_{n\nu}] = \delta_{\mu,\nu} \delta_{m,n}. \tag{12}$$

The new label $\nu = \pm 1$ refers to mass and component fluctuations.

The bosonic version of the unperturbed Hamiltonian in the N-fermion sector is [32,36]

$$\tilde{H}_0 = \frac{\hbar\omega_\ell}{2} \sum_{m>0,\nu} m\{\hat{d}^\dagger_{m\nu} \hat{d}_{m\nu} + \hat{d}_{m\nu} \hat{d}^\dagger_{m\nu}\}. \tag{13}$$

The complete bosonic interaction operator becomes

$$\begin{aligned} \hat{V} &= \frac{1}{2} \sum_{m>0,\nu} m[V_{a\parallel}(m) + \nu\, V_{a\perp}(m)]\{\hat{d}^\dagger_{m\nu} \hat{d}_{m\nu} + \hat{d}_{m\nu} \hat{d}^\dagger_{m\nu}\} \\ &\quad + \frac{1}{2} \sum_{m>0,\nu} m[V_{b\parallel}(m) + \nu\, V_{b\perp}(m)]\{\hat{d}^{\dagger 2}_{m\nu} + \hat{d}^2_{m\nu}\}. \end{aligned} \tag{14}$$

The total bosonic Hamiltonian is diagonalized in a standard way using the Bogoliubov transformation

$$\hat{d}_{m\nu} = \hat{S}^\dagger \hat{f}_{m\nu} \hat{S} = \hat{f}_{m\nu} \cosh \zeta_{m\nu} - \hat{f}^\dagger_{m\nu} \sinh \zeta_{m\nu}, \tag{15}$$

with

$$\hat{S} = \exp\left\{ \frac{1}{2} \sum_{m>0,\nu=\pm 1} \zeta_{m\nu} (\hat{f}^2_{m\nu} - \hat{f}^{\dagger 2}_{m\nu}) \right\}. \tag{16}$$

The transformation parameters $\zeta_{m\nu}$ are determined by the diagonalization conditions

$$\tanh(2\zeta_{m\nu}) = \frac{V_{b\parallel}(m) + \nu\, V_{b\perp}(m)}{\hbar\omega_\ell + V_{a\parallel}(m) + \nu V_{a\perp}(m)}. \tag{17}$$

Finally, we arrive at the free bosonic Hamiltonian

$$\tilde{H} = \sum_{m>0,\nu} m\, \epsilon_{m\nu} \hat{f}^\dagger_{m\nu} \hat{f}_{m\nu} + \text{const}, \tag{18}$$

describing density wave excitations in the two-component Fermi gas. The excitation spectra are

$$\epsilon_{m\nu}=\frac{\hbar\omega_{\ell}+V_{a\parallel}(m)+\nu V_{a\perp}(m)}{\cosh(2\zeta_{m\nu})}. \tag{19}$$

In connection with the calculation of one-particle matrix elements, scaled coupling constants

$$\alpha_{m\nu}\equiv\frac{1}{2}\sinh(2\zeta_{m\nu}),\quad \gamma_{m\nu}\equiv\sinh^2\zeta_{m\nu} \tag{20}$$

will appear.

Usually, the intracomponent scattering is negligible ($V_{\parallel}\to 0$, the case $V_{\parallel}\neq 0$ was considered in [24] for the one-component system) and dominant forward scattering for the intercomponent part results [35] in

$$V_{a\perp}(m)=V_{b\perp}(m)\equiv V(m)\hbar\,\omega_{\ell}. \tag{21}$$

Then the simpler relations

$$\epsilon_{m\nu}=\hbar\omega_{\ell}\sqrt{1+2\nu V(m)},\quad \alpha_{m\nu}=\frac{\nu V(m)}{2\sqrt{1+2\nu V(m)}} \tag{22}$$

hold for $|V(m)|<\hbar\omega_{\ell}/2$.

Following [24], we will also consider two specific interaction models: A simplified model IM1, when only one mode $V(m)=V(1)(\delta_{m,1}+\delta_{m,-1})$ contributes. This model preserves many of the features of the interaction in the full model (interaction model 2, see IM2 below), when infinitely many modes are superimposed.

In the case of IM1, the relevant coupling constants are

$$\zeta_{1\nu}=\frac{1}{2}\operatorname{artanh}\left(\frac{\nu V(1)}{1+\nu V(1)}\right),\quad \alpha_{1\nu}=\frac{1}{2}\sinh(2\zeta_{1\nu}),$$

$$\gamma_{1\nu}=\frac{1}{2}(\sqrt{1+4\alpha_{1\nu}^2}-1). \tag{23}$$

In the case of IM2, the coupling constants decay exponentially according to

$$\alpha_{m\nu}=\exp(-r_{\alpha}m/2)\alpha_{0\nu},\quad \alpha_{0\nu}=\exp(r_{\alpha}/2)\alpha_{1\nu},$$

$$\gamma_{m\nu}=\exp(-r_{\gamma}m)\gamma_0,\quad \gamma_{0\nu}=\exp(r_{\gamma})\gamma_{1\nu}. \tag{24}$$

An essential step in the actual calculation of physical quantities is the connection between fermionic operators and bosonic fields. The bosonization of fermion generation and destruction operators is completely solved for the Luttinger model [32,37–39].

In the present case, the situation is less comfortable: Apart from the above association of mass and component fluctuation operators with the $\hat{d}$ operators, we can bosonize only bilinear forms of an auxiliary field following the prescription of [40]. The auxiliary field is defined by

$$\hat{\psi}_{a\sigma}(v)\equiv\sum_{l=-\infty}^{\infty}e^{ilv}\hat{c}_{l\sigma}=\hat{\psi}_{a\sigma}(v+2\pi). \tag{25}$$

The Appendix demonstrates that the required bosonization for a two-component Fermi gas is

$$\hat{\psi}_{a\sigma}^{\dagger}(u)\hat{\psi}_{a\sigma}(v)=G_N(u-v)\exp\{-i[\hat{\phi}_{\sigma}^{\dagger}(u)-\hat{\phi}_{\sigma}^{\dagger}(v)]\}\times\exp\{-i[\hat{\phi}_{\sigma}(u)-\hat{\phi}_{\sigma}(v)]\}, \tag{26}$$

using the two-component non-Hermitian bosonic field

$$\hat{\phi}_{\sigma}(v)=-i\sum_{n=1}^{\infty}\frac{1}{\sqrt{2n}}e^{inv}(\hat{d}_{n+}+\sigma\hat{d}_{n-})\neq\hat{\phi}_{\sigma}^{\dagger}(v). \tag{27}$$

The distribution-valued prefactor $G_N(u)$ is the same as in [40]:

$$G_N(u)=\sum_{l=-\infty}^{N-1}e^{-il(u+i\eta)}. \tag{28}$$

III. ONE-PARTICLE MATRIX ELEMENTS

The above prescription allows us to calculate analytically all m-particle matrix elements of bilinear fermion operators. It is not difficult to carry the calculation of one-particle matrix elements in [24] over to the present case of two components:

$$\langle\hat{c}_{n\sigma}^{\dagger}\hat{c}_{q\sigma}\rangle=\sum_{l=-\infty}^{N-1}\int_0^{2\pi}\int_0^{2\pi}\frac{du\,dv}{4\pi^2}e^{i(n-l)(u+i\epsilon)-i(q-l)(v-i\epsilon)}\times\langle e^{-i\hat{\phi}_{\sigma}^{\dagger}(u)+i\hat{\phi}_{\sigma}^{\dagger}(v)}e^{-i\hat{\phi}_{\sigma}(u)+i\hat{\phi}_{\sigma}(v)}\rangle. \tag{29}$$

Using the bosonic Wick theorem, the expectation value $\langle\ \rangle\equiv\exp[-W_{\sigma}]$ on the right-hand side can be evaluated. At zero temperature, the function W_{σ} is given by

$$W_{\sigma}=W_{\sigma}(u,v)=\sum_{\nu}\sum_{m=1}^{\infty}\frac{1}{m}[\gamma_{m\nu}-\alpha_{m\nu}\cos m(u+v)]\times\{1-\cos m(u-v)\}. \tag{30}$$

This quantity is independent of component label σ, as expected.

Comparing Eq. (30) with Eq. (39) in [24], it is seen that the effective coupling constants in the two-component case are

$$\bar{\alpha}_m=\frac{1}{2}\sum_{\nu=1}^{2}\alpha_{m\nu},\quad \bar{\gamma}_m=\frac{1}{2}\sum_{\nu=1}^{2}\gamma_{m\nu}. \tag{31}$$

W is a real and even function of its arguments leading to the symmetries

$$\langle\hat{c}_{n\sigma}^{\dagger}\hat{c}_{q\sigma}\rangle=\langle\hat{c}_{q\sigma}^{\dagger}\hat{c}_{n\sigma}\rangle=\langle\hat{c}_{n\sigma}^{\dagger}\hat{c}_{q\sigma}\rangle^{*} \tag{32}$$

and to the condition $n+q=2m,\ m=0,1,2,\ldots$.

For the interaction model IM1, one of the integrations in Eq. (30) can be performed giving the closed expression for the matrix elements of each component:

$$M(m,p)\equiv\langle\hat{c}^{\dagger}_{m-p}\hat{c}_{m+p}\rangle=\frac{1}{2}\,\delta_{p,0}-\frac{1}{2\pi}\int_{-\pi}^{\pi}ds\left\{\frac{\sin[(m+1/2-N)s]}{2\,\sin(s/2)}\right\}\times\exp\{-2\,\overline{\gamma}_1[1-\cos(s)]\}\times I_p\{2\,\overline{\alpha}_1[1-\cos(s)]\}. \quad (33)$$

Due to the factor $\{\sin(\ldots)\}$, the following symmetries hold:

$$\langle\hat{c}^{\dagger}_{2N-1-m-p\;\sigma}\hat{c}_{2N-1-m+p\;\sigma}\rangle=\delta_{p,0}-\langle\hat{c}^{\dagger}_{m-p\;\sigma}\hat{c}_{m+p\;\sigma}\rangle. \quad (34)$$

Similarily, IM2 leads to

$$M(m,p)=\frac{1}{2}\,\delta_{p,0}-\int_{-\pi}^{\pi}\frac{dt}{2\pi}\,\frac{\cos(p\,t)}{[1+Z_\alpha-\cos(t)]^{\overline{\alpha}_0}}\times\int_{-\pi}^{\pi}\frac{ds}{2\pi}\left\{\frac{\sin[(m+1/2-N)s]}{2\,\sin(s/2)}\right\}\times\left[\frac{Z_\gamma}{1+Z_\gamma-\cos(s)}\right]^{\overline{\gamma}_0}\{[1+Z_\alpha-\cos(t-s)]\times[1+Z_\alpha-\cos(t+s)]\}^{\overline{\alpha}_0/2}, \quad (35)$$

with decay parameters

$$Z_\gamma=\cosh(r_\gamma)-1,\quad Z_\alpha=\cosh(r_\alpha/2)-1. \quad (36)$$

IV. NUMERICAL RESULTS

The main results of the paper are the formulas (33) and (35) for the one-particle matrix elements. They are identical in form to those in [24], however they depend differently on the coupling constants. This leads to very different physical predictions, which are presented in a number of figures for fermion numbers $2N=14+14$.

Using Eqs. (17) and (20), it is found that the main coupling parameters $\overline{\alpha}_m$,

$$\overline{\alpha}_m=\frac{V(m)}{4}\left\{\frac{1}{\sqrt{1+2\,V(m)}}-\frac{1}{\sqrt{1-2\,V(m)}}\right\}, \quad (37)$$

are nonpositive and even functions of the interactions $V(m)$: Irrespective of the sign of the interaction between the two components, the effective interaction in each component of the Fermi gas is attractive.

In the case of IM1, only $\overline{\alpha}_1$ is needed as an input parameter in the calculation of the matrix elements. $|V(1)|$ is obtained via Eq. (37) and all other quantities such as $\zeta_{1\nu}$ and $\overline{\gamma}_1$ can be calculated from Eqs. (23) and (31).

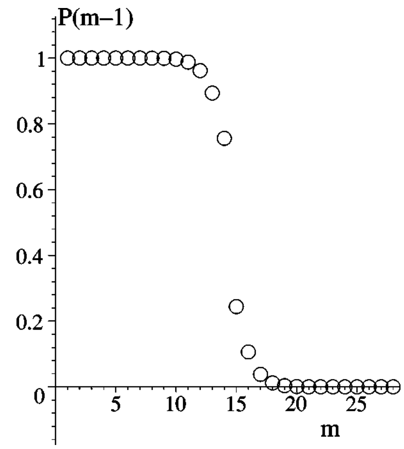

FIG. 1. Occupation probabilities P of oscillator states $m-1$ ($m=1,2,\ldots$) for an interacting two-component Fermi gas of $2N=14+14$ atoms in a one-dimensional harmonic trap at zero temperature. Interaction model 1 with $\overline{\alpha}_1=-1$ has been used.

We start with the discussion of the occupation probabilities $P(m)\equiv M(m,p=0)$ of oscillator states as shown in Fig. 1. It is seen that interactions smooth out the Fermi edge at $m_F=N-1$, but still leave a gap (not an energy gap) at m_F.

Figure 2 displays the off-diagonal matrix elements for $p=1$. They are significant near the Fermi edge $m_F=N-1$ and cannot be neglected. Their values increase further with increasing coupling strength.

We also present results for the particle density and the momentum density. Both are expected to show Friedel oscillations [41] as noted in [24,34]. In agreement with [24], the effective intracomponent interaction, which is always attractive, suppresses the Friedel oscillations in the particle density,

$$n(z)=\sum_{m=0}^{\infty}\sum_{p=-m}^{m}\psi_{m-p}(z)\psi_{m+p}(z)M(m,p), \quad (38)$$

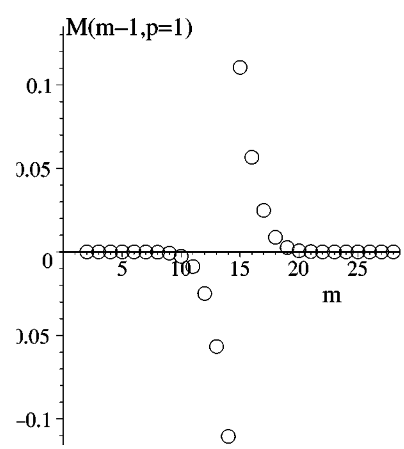

FIG. 2. Off-diagonal matrix elements M versus oscillator state $m-1$ ($m=1,2,\ldots$) for an interacting two-component Fermi gas of $2N=14+14$ atoms in a one-dimensional harmonic trap at zero temperature. Interaction model 1 with $\overline{\alpha}_1=-1$ has been used.

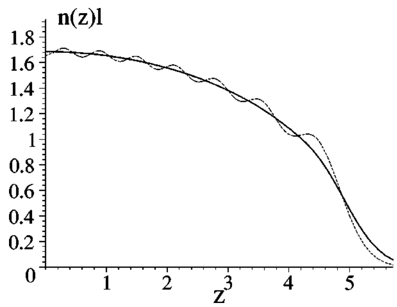

FIG. 3. Dimensionless particle density $n(z)\ell$ (ℓ is the oscillator length) versus dimensionless distance z from the center of the one-dimensional harmonic trap for $2N=14+14$ atoms in the two-component Fermi gas at zero temperature. The broken curve shows unperturbed Friedel oscillations. The smooth curve refers to the interacting case with $\overline{\alpha}_1=-1$. Interaction model 1 has been used.

as is seen in Fig. 3. In Eq. (38), $\psi_m(z)$ is the oscillator state $|m\rangle$ in position representation.

Conversely, the Friedel oscillations in the momentum density

$$p(k)=\sum_{m=0}^{\infty}\sum_{p=-m}^{m}(-1)^p\psi_{m-p}(k)\psi_{m+p}(k)M(m,p) \tag{39}$$

are enhanced [24]. This is displayed in Fig. 4 for strong coupling ($\overline{\alpha}_1=-10$). We have chosen the oscillator length $\ell\equiv\sqrt{\hbar/(m_A\omega_\ell)}$ as the unit of length, rendering $n(z)$ and z as well as $p(k)$ and k dimensionless.

In the case of IM2, some modifications occur. We again set $\overline{\alpha}_1=-1$. We need $\overline{\alpha}_m$ and $\overline{\gamma}_m(m=0,1,2\ldots)$ for the evaluation of Eq. (35). This requires knowledge of the decay constants r_α and r_γ [cf. Eq. (24)]. For convenience, we set $r_\alpha=r_\gamma\equiv r$ and estimate r by the following argument.

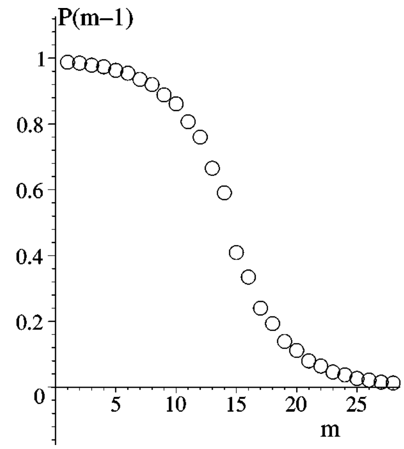

FIG. 5. Occupation probabilities P of oscillator states $m-1$ ($m=1,2,\ldots$) for an interacting two-component Fermi gas of $2N=14+14$ atoms in a one-dimensional harmonic trap at zero temperature. Interaction model 2 with $\overline{\alpha}_0=-1.16$ has been used.

The minimum wave number increment in the trap is $\Delta k\approx 1/L_F\propto 1/\sqrt{N}$, where $L_F=\sqrt{2N-1}$ is the half-width of the classically allowed region at the Fermi energy. We therefore set $r\approx 1/\sqrt{N}$ or roughly $r=0.3$ for the present case $N=14$. This gives $\overline{\alpha}_0=-1.16$ for $\overline{\alpha}_1=-1$ and $\overline{\gamma}_0=1.19$.

Figure 5 shows the occupation probabilities of oscillator states for IM2. It is seen that they are more smoothly distributed than in the case of IM1, but still leave a gap at the Fermi edge.

Finally, we show the momentum density for IM2 in Fig. 6. The Friedel oscillations are still recognizable for small momenta, but strongly suppressed for momenta approaching $k_F=\sqrt{2N-1}$.

The off-diagonal matrix elements are significantly smaller for IM2 than for IM1. Nevertheless, they cannot be ne-

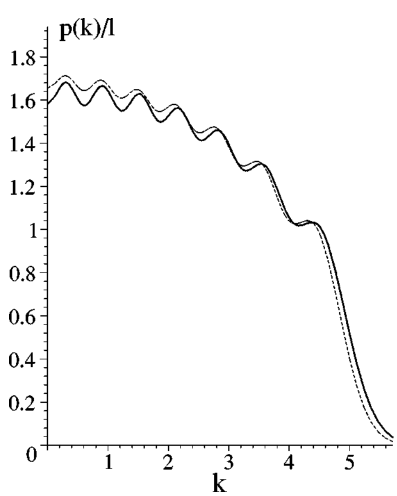

FIG. 4. Dimensionless momentum density $p(k)/\ell$ (ℓ is the oscillator length) versus dimensionless momentum k for $2N=14+14$ atoms of a two-component Fermi gas in a one-dimensional harmonic at zero temperature. The broken curve shows unperturbed Friedel oscillations. The thick curve refers to the interacting case with $\overline{\alpha}_1=-10$. Interaction model 1 has been used.

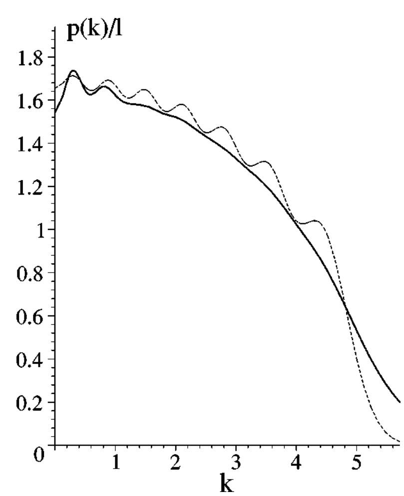

FIG. 6. Dimensionless momentum density $p(k)/\ell$ (ℓ is the oscillator length) versus dimensionless momentum k for $2N=14+14$ atoms of a two-component Fermi gas in a one-dimensional harmonic at zero temperature. The broken curve shows unperturbed Friedel oscillations. The thick curve refers to the interacting case with $\overline{\alpha}_0=-1.16$. Interaction model 2 has been used.

glected: By comparing Eq. (38) with Eq. (39), it is seen that particle and momentum density would coincide in such an approximation.

V. FERMI EDGE

Figure 1 and also Fig. 5 do not show the gapless distribution of occupation probabilities near the Fermi edge $m_F = N-1$, which is characteristic of a Luttinger liquid, i.e., our system is not a Luttinger liquid. This cannot be expected because the system is finite. We can, however, get a glimpse at Luttinger liquid behavior in a special limit, which also presupposes a large particle number N.

First, we consider a very slow decay of the interaction modes $V(m)$ in IM2, i.e., $r_\alpha \to r_\gamma \ll 1$. The factor

$$\left[\frac{Z_\gamma}{1+Z_\gamma-\cos(s)}\right]^{\overline{\gamma}_0} \to \left(\frac{r_\gamma^2}{r_\gamma^2+s^2}\right)^{\overline{\gamma}_0} \tag{40}$$

in the large square brackets of the integrand in Eq. (35) then becomes sharply localized at $s=0$.

We now calculate the occupation probability $P(\Delta k_n)$,

$$\langle \hat{c}^\dagger_{N-1+n}\hat{c}_{N-1+n}\rangle = \langle \hat{c}^\dagger_{\Delta k_n}\hat{c}_{\Delta k_n}\rangle \equiv P(\Delta k_n) \tag{41}$$

near the Fermi edge and for $N \gg 1$. $P(\Delta k_n)$ becomes a quasicontinuous function of the wave-number deviation $\Delta k_n = k_n - k_F = n/L_F \to \Delta k$, provided $|n| \ll \min(N, 1/r_\gamma)$ is fulfilled. Using Eq. (40) in Eq. (35), we obtain

$$P(\Delta k) = \frac{1}{2} - \left\{ {}_3F_2\left[\overline{\gamma}_0, \frac{1}{2}, 1; 1, \frac{3}{2}; -\left(\frac{\pi}{r_\gamma}\right)^2\right] r_\gamma L_F \right\} \Delta k \tag{42}$$

in terms of a generalized hypergeometric function. It is seen that $P(\Delta k)$ depends linearly on the wave-number deviation in a small region near the Fermi edge.

This can be compared with the Luttinger liquid prediction (cf. e.g., [26])

$$P_{LL}(\Delta k) = \frac{1}{2} - \mathrm{sgn}(\Delta k) C |\Delta k|^\beta. \tag{43}$$

C is a constant and the exponent β depends on the Luttinger liquid coupling strength γ_{LL} according to

$$\beta = 2\gamma_{LL} \quad \text{for} \quad \gamma_{LL} < \frac{1}{2} \tag{44}$$

and

$$\beta = 1 \quad \text{for} \quad \gamma_{LL} \geq \frac{1}{2}. \tag{45}$$

We conclude that the above limit of our model agrees with the case $\gamma_{LL} \geq 1/2$ of the Luttinger liquid.

VI. DISCUSSION AND SUMMARY

For the interaction to become significant in the quantities calculated, its strength $V(1)$ should be as large as $|V(1)| \lesssim 0.5$. We demonstrate that this condition is within experimental reach.

To this order, we consider the dipole-dipole interaction [15]. It is marginally long-ranged and thus favors forward scattering. In [35], it is shown that the intercomponent interaction between longitudinally aligned dipoles reduces exactly to the effective one-dimensional potential

$$\tilde{V}_{1\mathrm{D}}(k) = -\frac{\mu_0 \mu^2 \alpha_t^2}{2\pi}\left[1 + \frac{k^2}{2\alpha_t^2}\exp\left(\frac{k^2}{2\alpha_t^2}\right)\mathrm{Ei}\left(-\frac{k^2}{2\alpha_t^2}\right)\right]$$

in momentum space. Here, α_t is the inverse of the transverse oscillator length, μ the magnetic dipole moment, and Ei denotes the exponential integral.

Using this equation in the exact formula (A13) in [24], $V(1)$ for $N=14$ is found to be

$$V(1) = -0.8\left(\frac{\mu_0 \mu^2 m_A^{3/2} \omega_{\not\,}^{1/2}}{2\pi\hbar^{5/2}}\right)\frac{1}{F}.$$

The quantity F denotes the filling factor $F = N\omega_{\not\,}/\omega_t$. For example in ^{53}Cr, $V(1)$ becomes of the required magnitude provided F is very small, i.e., the trap is highly anisotropic.

In summary, the bosonization method has been used to construct a theory for a two-component gas of spin-polarized fermions in a one-dimensional harmonic potential with forward scattering between the two components. Asymptotic results with respect to the fermion number N were obtained for the one-particle matrix elements and used to discuss occupation probabilities for oscillator states, off-diagonal matrix elements, and distribution functions for particles and momenta in the harmonic trap. All these quantities can be significantly affected by the attractive interaction generated within each component. Specifically, the Friedel oscillations in the particle density are suppressed, while they survive in the momentum density.

It remains to be seen whether the predicted Friedel oscillations can be observed experimentally. The amplitudes of the Friedel oscillations scale as $1/N$ [34], hence Friedel oscillations are unobservable in a macroscopic bounded Fermi sea. Small particle numbers pose, however, severe detection problems. A conceivable experimental method to observe Friedel oscillations for atom numbers of the order of 100 is indicated in [34]. The method proposes microfabrication techniques to produce arrays of microtraps.

On the other hand, the asymptotic bosonization method requires particle numbers, which are not too small. This is due to the presence of the anomalous vacuum, which couples to the real particles. For instance, the sum rule $\Sigma_n P(n) = N$ gives a somewhat larger value than the number N of real particles when Eq. (33) or Eq. (35) is used. The excess $\Delta N > 0$ grows with coupling strength and decreasing particle number. For $N=14$ and very strong coupling $\overline{\alpha_1}=-10$, ΔN is about 8×10^{-3}; for $\overline{\alpha_1}=-1$, ΔN is less than 10^{-10}.

The atom number $2N=14+14$ and the coupling values employed here are appropriate to give visible Friedel oscillations and reliable results of the bosonization method.

ACKNOWLEDGMENTS

The authors thank S. N. Artemenko, F. Gleisberg, and W. P. Schleich for valuable discussions and the Deutsche Forschungsgemeinschaft for financial support.

APPENDIX

In this appendix, we extend the bosonization procedure in [40] to the case of two components. Instead of $\hat{d}_{p\pm}$ operators, which are needed for the diagonalization of the interacting Hamiltonian, the following set of operators plays the role of the $\hat{b}$ and $\hat{b}^+$ operators ($n\geqslant1$) in [40]:

$$\hat{b}^\dagger_{n\sigma}\equiv\frac{1}{\sqrt{2}}[\hat{d}^\dagger_{n+}+\sigma\hat{d}^\dagger_{n-}],\quad \hat{b}_{n\sigma}\equiv\frac{1}{\sqrt{2}}[\hat{d}_{n+}+\sigma\hat{d}_{n-}]. \tag{A1}$$

They are canonical conjugates. Evidently

$$\hat{b}^\dagger_{n\sigma}\equiv\frac{1}{\sqrt{n}}\hat{\rho}_\sigma(n). \tag{A2}$$

Then the two relations hold,

$$[\hat{b}^\dagger_{n\sigma},\hat{c}^\dagger_{k\sigma'}\hat{c}_{l\sigma'}]=\delta_{\sigma,\sigma'}\frac{1}{\sqrt{n}}(\hat{c}^\dagger_{k+n\sigma}\hat{c}_{l\sigma}-\hat{c}^\dagger_{k\sigma}\hat{c}_{l-n\sigma}),$$
$$[\hat{b}_{n\sigma},\hat{c}^\dagger_{k\sigma'}\hat{c}_{l\sigma'}]=\delta_{\sigma,\sigma'}\frac{1}{\sqrt{n}}(\hat{c}^\dagger_{k-n\sigma}\hat{c}_{l\sigma}-\hat{c}^\dagger_{k\sigma}\hat{c}_{l+n\sigma}). \tag{A3}$$

Following the arguments in [40], the associated Bose fields for $\sigma=\sigma'$ are

$$\hat{\phi}_\sigma(v)=-i\sum_{n=1}^{\infty}\frac{1}{\sqrt{n}}e^{inv}\hat{b}_{n\sigma}\equiv-i\sum_{n=1}^{\infty}\frac{1}{\sqrt{2n}}e^{inv}(\hat{d}_{n+}+\sigma\hat{d}_{n-})\neq\hat{\phi}^\dagger_\sigma(v). \tag{A4}$$

[1] M.H. Anderson *et al.*, Science **269**, 198 (1995); K.B. Davis *et al.*, Phys. Rev. Lett. **75**, 3969 (1995); C.C. Bradley *et al.*, *ibid.* **75**, 1687 (1995).
[2] F. Brosens, J.T. Devreese, and L.F. Lemmens, Phys. Rev. E **57**, 3871 (1998).
[3] G.M. Bruun and K. Burnett, Phys. Rev. A **58**, 2427 (1998).
[4] M.A. Zaluska-Kotur, M. Gajda, A. Orlowski, and J. Mostowski, Phys. Rev. A **61**, 033613 (2000).
[5] M. Houbiers *et al.*, Phys. Rev. A **56**, 4864 (1997).
[6] M.A. Baranov and D.S. Petrov, Phys. Rev. A **58**, R801 (1998).
[7] M. Houbiers and H.T.C. Stoof, Phys. Rev. A **59**, 1556 (1999).
[8] R. Combescot, Phys. Rev. Lett. **83**, 3766 (1999).
[9] B. DeMarco and D.S. Jin, Science **285**, 1703 (1999).
[10] F. Schreck *et al.*, Phys. Rev. A **64**, 011402(R) (2001).
[11] V. Vuletic *et al.*, Phys. Rev. Lett. **80**, 1634 (1998).
[12] J. Fortagh, A. Grossmann, C. Zimmermann, and T.W. Hänsch, Phys. Rev. Lett. **81**, 5310 (1998).
[13] J. Denschlag, D. Cassettari, and J. Schmiedmayer, Phys. Rev. Lett. **82**, 2014 (1999).
[14] J. Reichel, W. Hänsel, and T.W. Hänsch, Phys. Rev. Lett. **83**, 3398 (1999).
[15] K. Goral, B-G. Englert, and K. Rzazewski, Phys. Rev. A **63**, 033606 (2001).
[16] H.L. Bethlem *et al.*, Nature (London) **406**, 491 (2000).
[17] J.L. Cardy, J. Phys. A **17**, L385 (1984).
[18] S. Eggert and I. Affleck, Phys. Rev. B **46**, 10 866 (1992).
[19] M. Fabrizio and A.O. Gogolin, Phys. Rev. B **51**, 17 827 (1995).
[20] R. Egger and H. Grabert, Phys. Rev. Lett. **75**, 3505 (1995).
[21] Y. Wang, J. Voit, and Fu-Cho Pu, Phys. Rev. B **54**, 8491 (1996).
[22] A.E. Mattsson, S. Eggert, and H. Johannesson, Phys. Rev. B **56**, 15 615 (1997).
[23] J. Voit, Yupeng Wang, and M. Grioni, Phys. Rev. B **61**, 7930 (2000).
[24] W. Wonneberger, Phys. Rev. A **63**, 063607 (2001).
[25] V. J. Emery, in *Highly Conducting One-Dimensional Solids*, edited by J.T. Devreese, R.P. Evard, and V.E. van Doren (Plenum, New York, 1979), p. 247.
[26] J. Voit, Rep. Prog. Phys. **58**, 977 (1995).
[27] H.J. Schulz, *Fermi Liquids and Non-Fermi Liquids*, in *Mesoscopic Quantum Physics*, edited by E. Akkermans, G. Montambaux, J.-L. Pichard, and J. Zinn-Justin (Elsevier, Amsterdam, 1995), p. 533.
[28] A. Luther and V.J. Emery, Phys. Rev. Lett. **33**, 589 (1974).
[29] I.E. Dzyaloshinskii and A.I. Larkin, Zh. Éksp. Teor. Fiz. **65**, 411 (1973) [Sov. Phys. JETP **38**, 202 (1974)].
[30] H.C. Fogedby, J. Phys. C **9**, 3757 (1976).
[31] G. Grinstein, P. Minnhagen, and A. Rosengren, J. Phys. C **12**, 1271 (1979).
[32] F.D.M. Haldane, J. Phys. C **14**, 2585 (1981).
[33] P. Vignolo, A. Minguzzi, and M.P. Tosi, Phys. Rev. Lett. **85**, 2850 (2000).
[34] F. Gleisberg, W. Wonneberger, U. Schlöder, and C. Zimmermann, Phys. Rev. A **62**, 063602 (2000).
[35] F. Gleisberg and W. Wonneberger (unpublished).
[36] R. de L. Kronig, Physica (Amsterdam) **2**, 968 (1935).
[37] A. Luther and I. Peschel, Phys. Rev. B **9**, 2911 (1974).
[38] D.C. Mattis, J. Math. Phys. **15**, 609 (1974).
[39] R. Heidenreich, R. Seiler, and D.A. Uhlenbrock, J. Stat. Phys. **22**, 27 (1980).
[40] K. Schönhammer and V. Meden, Am. J. Phys. **64**, 1168 (1996).
[41] J. Friedel, Nuovo Cimento, Suppl. **7**, 287 (1958).